Available online at www.sciencedirect.com

ScienceDirect

Ceramics International 39 (2013) 8885–8892

CERAMICS INTERNATIONAL

www.elsevier.com/locate/ceramint

The preparation and properties of zirconia-doped Y–Si–Al–O–N oxynitride glasses and glass-ceramics

Gao Qu, Zhiwei Luo, Weizhen Liu, Anxian Lu*

School of Material Science and Engineering, Central South University, Changsha 410083, PR China

Received 8 February 2013; received in revised form 24 March 2013; accepted 24 April 2013
Available online 1 May 2013

Abstract

Two series (N-9 and N-18 series) of zirconia-doped Y–Si–Al–O–N oxynitride glasses and glass-ceramics were designed. Nominal compositions of the glass samples in equivalent percent (eq%) are *x*Zr: (24–0.25*x*)Y: (15–0.25*x*)Al: (61–0.5*x*)Si: 91O: 9 N and *x*Zr: (24–0.25*x*)Y: (15–0.25*x*)Al: (61–0.5*x*)Si: 82O: 18 N ($x=0$, 2, 4, 6), respectively. The obtained samples were characterized by differential thermal analysis (DTA), X-ray diffraction (XRD), fourier transform infrared spectroscopy (FTIR) and scanning electron microscopy (SEM). Densities, Vickers hardness, fracture toughness, glass transition temperature, and thermal expansion coefficient data were established for each sample. Effect of Zr and N content on glass network structure, thermal and mechanical properties was investigated. It was found that the addition of zirconia is effective in preparing Y–Si–Al–O–N oxynitride glasses with lower glass transition temperature and higher hardness.

Keywords: C. Mechanical properties; Oxynitride glass-ceramics; Zirconia-doped; Oxynitride glass

1. Introduction

Oxynitride glasses have been studied intensively because of their excellent structure and properties. In recent years, particular interest has been focused on the Y–Si–Al–O–N system [1–4], where Y is a modifying cation. Y–Si–Al–O–N glasses formed at grain boundaries in Si_3N_4 and SiAlON ceramics are essentially alumino-silicate glasses in which nitrogen atoms substitute for oxygen atoms in the glass network. This substitution contributed to the formation of stronger covalent bonds among the nitrogen-containing phases and the improvement of some mechanical properties such as elastic moduli, hardness, strength and fracture toughness [2]. Unfortunately, compared to oxide glasses, oxynitride glasses are of limited transparency, having colors varying between pale gray and almost black. The transparency of oxynitride glasses has been the subject of many investigations [5–7], but this has not led to significant progress being made toward the production of fully transparent oxynitride glasses. The promising uses of the oynitride glass have been focused by some researchers, such as armor material, in particular as an anti-ballistic material [8], glass fiber [9] and so on.

Several investigations have been made in understanding the nature of the oxynitride glasses and how additive oxides made an effect on properties [7,10,11]. Zirconia has a beneficial effect of the martensitic tetragonal-to-monoclinic transformation on toughening brittle materials, so that the fracture toughness of oxynitride glass-ceramics could be increased by the addition of ZrO_2 [12]. However, no investigations on effect of zirconia addition on properties of Y–Si–Al–O–N glasses and glass-ceramics have been reported. In this paper, small quantities of ZrO_2 were added to Y–Si–Al–O–N glasses of similar cation compositions to study the effect of zirconia on microstructure and properties such as fracture toughness, glass transition temperature and microhardness.

2. Experimental procedure

Y_2O_3 (99.9%, A&C Rare Earth Materials Center, China), α-Si_3N_4 (99.7%, averaged particle size 0.2 μm; Sinopharm Chemical Reagent Co. Ltd., China), Al_2O_3 (99%, Xilong Chemical Co. Ltd., China), SiO_2 (99%, Xilong Chemical Co.

*Corresponding author. Tel.: +86 0731 88830351; fax: +86 0731 88877057.
E-mail addresses: axlu@csu.edu.cn, qg_881206csu@163.com (A. Lu).

0272-8842/$ - see front matter © 2013 Elsevier Ltd and Techna Group S.r.l. All rights reserved.
http://dx.doi.org/10.1016/j.ceramint.2013.04.082

Table 1
Nominal compositions of the zirconia-doped Y–Al–Si–O–N oxynitride glasses (eq%).

Sample	Y	Al	Zr	Si	O	N
N-9 series						
Zr0N9	24	15	0	61	91	9
Zr2N9	23.5	14.5	2	60	91	9
Zr4N9	23	14	4	59	91	9
Zr6N9	22.5	13.5	6	58	91	9
N-18 series						
Zr0N18	24	15	0	61	82	18
Zr2N18	23.5	14.5	2	60	82	18
Zr4N18	23	14	4	59	82	18
Zr6N18	22.5	13.5	6	59	82	18

Ltd., China), ZrO_2 (99%, Xilong Chemical Co. Ltd., China) were used as raw materials. α-Si_3N_4 powder contained free silicon (0.2%) and iron (200 ppm). For the preparation of four series of glass samples as seen in Table 1, a batch of 80 g was prepared and milled in isopropyl alcohol for 4 h using Al_2O_3 as milling media; afterward, the slurries were dried at 60 °C and then melted inside a silica crucible at 1600 °C for 2 h under N_2 atmosphere (0.1 MPa), using a heating rate of 5 °C/min. Subsequently, the samples were first cooled with a cooling rate of 25 °C/min until a temperature of 900 °C annealing for 1 h to remove internal stresses, and afterward the samples were cooled down with furnace cooling to room temperature.

The microstructure of the samples was observed with the Scanning electron microscopy (SEM) and energy dispersive X-ray spectroscopy (EDS) using a FEI Quanta 200 ESEM, which was fitted with Peltier-cooled stage during ESEM operation. X-ray diffraction (XRD) was carried out in order to analyze the crystalline phase of the samples by an X-ray diffractometer (D/max 2500 model, Rigaku, Japan) with Cu-Kα radiation ($\lambda = 1.54178$ Å) operated at 40 kV and 50 mA. Data were collected from $2\theta = 10$–80° at a scanning rate of 8 deg./min.

The IR absorption spectra of glasses were carried out on the Thermo Scientific NICOLET 6700 spectrometers in the range of 400–4000 cm^{-1} using the KBr pellet technique. The samples were investigated as fine particles which were mixed with pulverized KBr in the ratio of 1:50 mg glass powder to KBr, respectively.

The density (ρ) was measured by the Archimedes method, using distilled water. Vickers hardness (H_v) tests were carried out on polished glass samples using a Matsuzawa micro-hardness tester Model MXT-a 1 with a pyramid shaped diamond indenter, applying loads between 4.9 and 9.8 N for 15 s. At least 10 measurements were taken for each sample. Indentation diagonals were measured to calculate hardness values in GPa. Fracture toughness (K_{Ic}) was measured by the indentation method with loads of 9.8 N and calculated according to the procedures given by Rouxel [13].

Differential thermal analysis (DTA, Rigaku TAS100, Japan) was carried out to determine the glass transition temperatures. About 10 mg powder sample was placed in an alumina crucible and heated at a rate of 5 °C/min up to 1300 °C under a flowing nitrogen atmosphere. Thermal expansion coefficient (α) was measured in a dilatometer (Netzsch, DIL402PC, Germany) in air at a heating and cooling rate of 5 °C/min and the thermal expansion coefficient was calculated between 50 and 500 °C.

3. Results and discussion

3.1. Glass formation

All prepared glasses samples are translucent and gray by the naked eye and it was observed that the color of the glass is darker as the amount of nitrogen content increases. The X-ray diffraction analysis confirmed that all the glasses are totally amorphous. Homogeneous microstructure of the glasses can be observed from the SEM.

A main obstacle for the utilization of the oxynitride glasses is its poor transparence in the visible region. Korgul et al. [14] have pointed out that the reason for the blackening of oxynitride glass is precipitation of silicon, which is assumed to result from the decomposition of Si_3N_4 or from the following reaction of Si_3N_4 with SiO_2.

$$Si_3N_4 + FeO \rightarrow SiO + FeSi_2 + 2N_{2(g)} \quad (1)$$

$$Si_3N_{4(s)} + SiO_{2(s)} \rightarrow 2SiO_{(g)} + 2Si_{(l)} + 2N_{2(g)} \quad (2)$$

Thus, in order to produce transparent oxynitride glass, extremely high purity starting materials are required and inert gas is used to protect the material from oxidation.

3.2. IR absorption spectrum

The room temperature FTIR absorption spectra of zirconia-doped Y–Si–Al–O–N glasses are shown in Fig. 3, where maxima of the broad band are marked. The IR absorption spectra of four N-9 glass samples (Zr0N9, Zr2N9, Zr4N9 and Zr6N9) in lower frequency (400–1400 cm^{-1}) are shown in Fig. 1(a) and four N-18 glass samples (Zr0N18, Zr2N18, Zr4N18 and Zr6N18) are shown in Fig. 1(b). There are about three bands which can be seen clearly in Fig. 1(a) and (b). The first broad band (800–1200 cm^{-1}) contains two absorption peaks located around 1080 cm^{-1} and 900 cm^{-1}. The second band (600–750 cm^{-1}) locates at about 650 cm^{-1}. The third band (400–600 cm^{-1}) contains two major peaks locating at about 460 cm^{-1} and 420 cm^{-1}. In N-9 glasses, the IR absorption band becomes broader with the increasing of Zr content. In addition, this trend can also be seen in the N-18 glasses. In order to show the effect of N content on glass structure clearly, Fig. 1(c) are plotted. As can be seen in Fig. 1(c), when the N content increases, a similar trend that the absorption band becomes broader comes to appear and the absorption band (800–1200 cm^{-1} and 400–600 cm^{-1}) becomes weaker.

The first band 800–1200 cm^{-1} is assigned to antisymmetric stretching vibrations of the Si–O–Si bonds within [SiO_4] tetrahedral. The occurrence of two maxima at around 1080 and 900 cm^{-1} and the shift toward the low frequencies of the

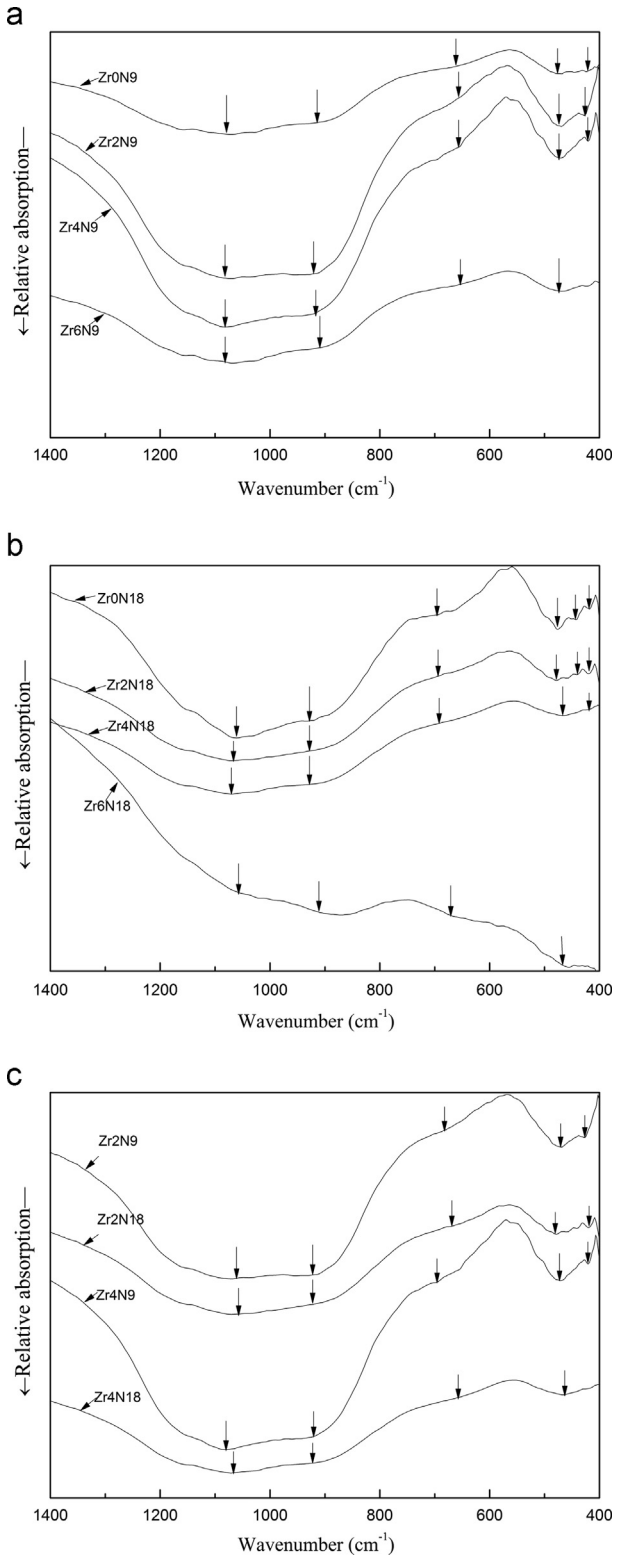

Fig. 1. Infrared absorption spectra of the zirconia-doped Y–Si–Al–O–N oxynitride glasses: (a) glass samples of Zr0N9, Zr2N9, Zr4N9 and Zr6N9, (b) glass samples of Zr0N18, Zr2N18, Zr4N18 and Zr6N18, (c) glass samples of Zr2N9, Zr2N18, Zr4N18 and Zr4N18.

absorption band can be attributed to $Si–O^-$ bond vibrations. The 1080 cm^{-1} absorption can be associated with Si–N vibrations and the 900 cm^{-1} can be Si–N–Si vibrations. The band 600–750 cm^{-1} is considered with SiO(Si, Al) symmetric stretching vibrations between the tetrahedral [15]. In the glass structure, the [SiO_4] tetrahedral are combined with four [AlO_4] tetrahedral and the absorption maxima of this line locates at ~680 cm^{-1}. The bands in 400–600 cm^{-1} region are due to bending vibrations of Si–O–Si and Si–O–Al linkages. The maximum of this band (about 460 cm^{-1} and 420 cm^{-1}) does not change its position with the change of zirconium ions but a broader band with the increase of Zr content has been observed and a similar situation also occurs on the first band (800–1200 cm^{-1}).

With the increasing of zirconium content, some ZrO_4 tetrahedral are present in the glass by partial Zr^{4+} ions participating in the formative network, which induces some Al^{3+} ions in six-fold coordination. Thus, the number of AlO_6 group increases and that of AlO_4 groups decreases, which leads to the decrease of the number of Al–O–Si bridging. In this case, the mixed environment around aluminum and silicon leads to the appearance of new vibration modes which are responsible for the widening of the absorption band (800–1200 cm^{-1} and 400–600 cm^{-1}). As can be seen from Fig. 1(c), with the increasing of N content, the bands (800–1200 cm^{-1} and 400–600 cm^{-1}) become broader and weaker. To the first band (800–1200 cm^{-1}), the increasing nitrogen content leads to the increase of the Si–N bonds which involves the weakening of the neighboring Si–O–(Si, Al) bonds with the appearance of υ(Si–N): around 1080 cm^{-1}, υ(N–Si–O): between 950 and 1000 cm^{-1}, υ(Si–N–Si): between 850 and 950 cm^{-1} vibration modes which make the band broader [16]. Similarly, in the third band (400–600 cm^{-1}), the increasing of Si–N bonds leads to the appearance of new vibration modes and also makes the band broader. In the second band (600–750 cm^{-1}), the characteristic band of AlO_4 tetrahedral becomes unconspicuous when nitrogen is incorporated in the glass. This modification could be considered to the decrease of aluminum in a four-fold coordination and to the partial replacement of oxygen atoms by nitrogen atoms around the AlO_4 tetrahedra. As is known to all, the IR spectrum absorption intensity is proportional to the square of the change of dipole moment in molecular vibration [17]. Because oxygen atoms have a higher electronegative than nitrogen atoms, the Si–O–Si bonds have a greater change of dipole moment than Si–N–Si bonds in molecular vibration. As a result, when nitrogen is added to the glass, the absorption bands (800–1200 cm^{-1} and 400–600 cm^{-1}) become weaker.

3.3. Density

The density of the glasses varies between 3.38 and 3.53 g/cm^3 (see Table 2). The variation of the density (ρ) as a function of zirconium content is shown in Fig. 2. As seen in Table 2, the density of the N-9 glass samples have values ranging from 3.38 to 3.47 g/cm^3, which the N-18 samples are ranging from 3.42 to 3.53 g/cm^3. The data thus indicate that the density (ρ) of the glasses depends both on N and Zr contents.

The increase of density with N content is in agreement with those of the previous studies [18,19]. The density is capable of investigating the changes in the structure of glasses and is

Table 2
properties of the zirconia-doped Y–Al–Si–O–N oxynitride glasses: color, density (ρ), thermal expansion coefficients (α, 50–500 °C), glass transition temperature (T_g), Vickers hardness (H_v), fracture toughness (K_{Ic}).

Sample ID	Color	ρ ($\pm$0.005 g/cm^3)	$\alpha_{(50-500\ ^\circ C)}$ ($\pm 0.05\times10^{-6}$ °C^{-1})	T_g ($\pm$5 °C)	H_v ($\pm$0.1 GPa)	K_{Ic} ($\pm$0.2 MPa m$^{1/2}$)
N-9 series						
Zr0N9	Pale gray	3.38	7.58	892	7.1	1.28
Zr2N9	Pale gray	3.43	6.31	889	7.7	1.31
Zr4N9	Pale gray	3.44	6.85	883	7.9	1.26
Zr6N9	Pale gray	3.47	6.24	882	7.8	1.29
N-18 series						
Zr0N18	Pale brown	3.42	7.01	935	8.1	1.55
Zr2N18	Pale brown	3.45	6.08	931	8.4	1.58
Zr4N18	Pale brown	3.49	6.28	929	8.4	1.54
Zr6N18	Pale brown	3.53	5.85	926	8.8	1.57

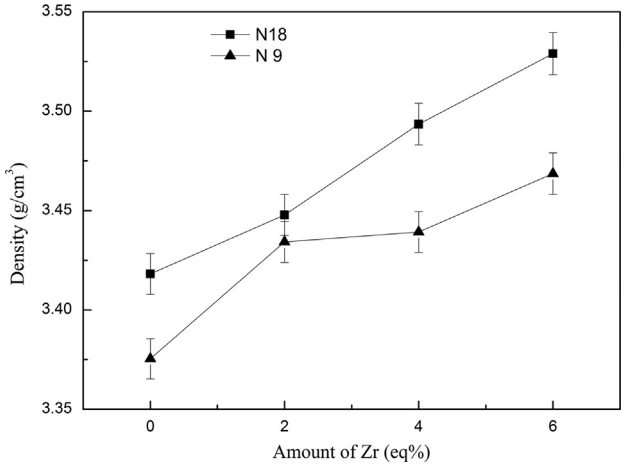

Fig. 2. Density of the zirconia-doped Y–Si–Al–O–N oxynitride glasses as a function of amount of zirconium.

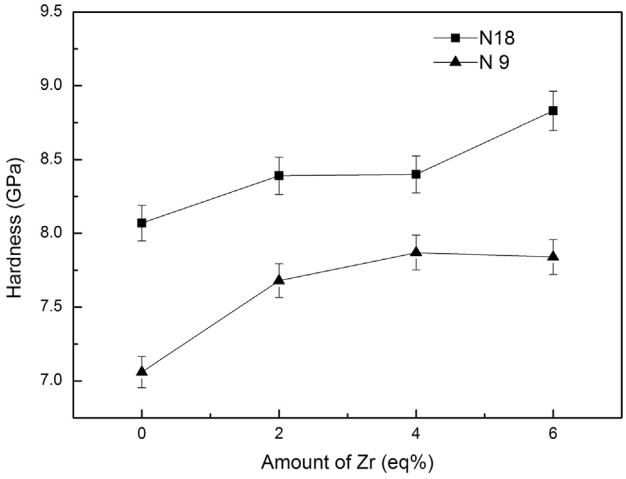

Fig. 3. Vickers hardness of the zirconia-doped Y–Si–Al–O–N oxynitride glasses as a function of amount of zirconium.

affected by structural softening or compactness, changes in coordination numbers, cross-link densities and dimensions of interstitial spaces of the glass system. The reason for the increase of density can be explained by the incorporation of tri-coordinated nitrogen, which makes the glass network more compact. Further, Zr atoms have a relatively great relative atomic mass which also leads to the increase of density.

3.4. Hardness and fracture toughness

Vickers hardness (H_v) and fracture toughness (K_{Ic}) values of the glass samples are listed in Table 2. Vickers hardness of each glass samples varies from 7.1 to 8.8 GPa and linearly increases with zirconium content. Furthermore, all N-18 glass samples with the same Zr content have a higher Vickers hardness than N-9 glass samples. As can be seen in Table 2, the value of fracture toughness varies from 1.26 to 1.58 MPa m$^{1/2}$ and has no much relationship with the zirconium content. However, the fracture toughness has a relationship with nitrogen content. The fracture toughness of N-18 glasses samples is better than those of N-9 glasses with same Zr content.

Only a small number of studies have previously been carried out on Zr-doped oxynitride glasses, the hardness for these, with

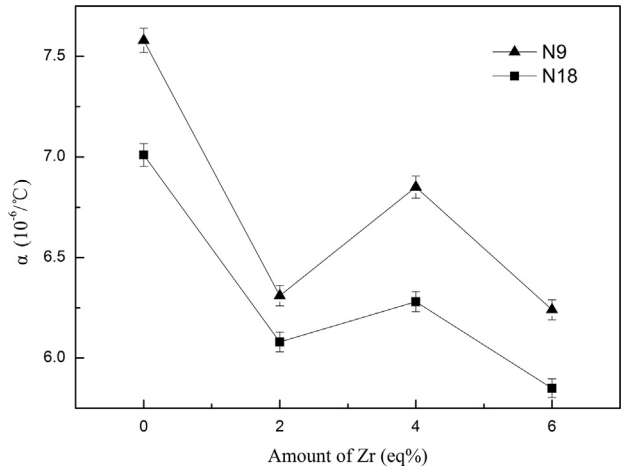

Fig. 4. Thermal expansion coefficient of the zirconia-doped Y–Si–Al–O–N oxynitride glasses as a function of amount of zirconium.

N content below 20 eq%, has been found to vary between 6 and 9 GPa [20]. Improvement of the Vickers hardness with nitrogen addition could also be owing to the formation of tri-coordinated nitrogen, which makes the oxynitride glasses more rigid. As can

be seen in Fig. 3, addition of Zr also has a positive effect on Vickers hardness of the oxynitride glasses. This is likely due to the solid solution effect of Zr within the glass structure which has a higher coordination number and cation field strength (CFS) [21]. The property changes follow usually linear dependence on ionic radii or CFS of the corresponding modifier elements [22]. In the analysis of TiO_2-doped Y–Si–Al–O–N glasses by Wakihara et al. [23], a similar trend for increasing H_v values with the incorporation of TiO_2 dopant was observed.

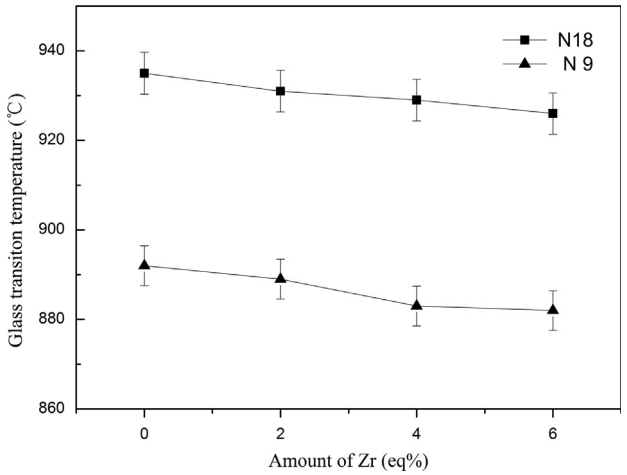

Fig. 5. Glass transition temperature (T_g) of the zirconia-doped Y–Si–Al–O–N oxynitride glasses as a function of amount of zirconium.

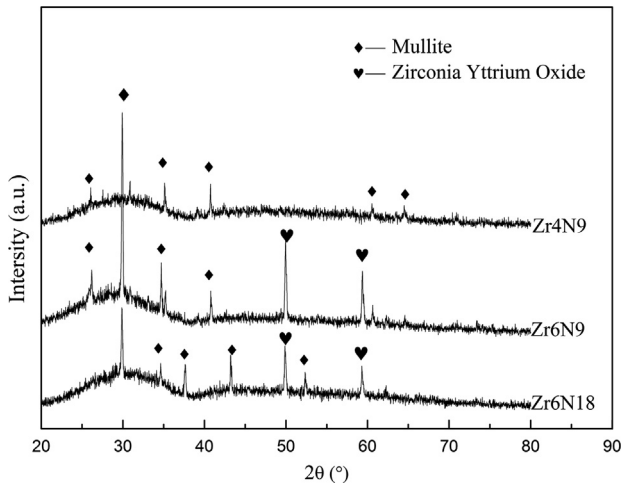

Fig. 6. XRD patterns of the zirconia-doped Y–Si–Al–O–N oxynitride glass-ceramic samples Zr4N9, Zr6N9 and Zr6N18.

Fracture toughness shows a great relationship with the nitrogen content from Table 2 while it does not show much relationship with the Zr content. The more rigid and stable oxynitride glass network is generally attributed to the replacement of bivalent O_2 atoms with trivalent N_2 atoms to create a more cross-linked glass structure and the increased resistance of the oxynitride glass to stress corrosion is often attributed to their increased durability and stability. Bhatnagar et al. [24] have already investigated the short crack behavior using indentation techniques to establish a reliable fracture toughness and to elucidate the anomalous densification behavior of the Y–Si–Al–O–N oxynitride glasses.

3.5. Thermal properties

The thermal expansion coefficient (α) and glass transition temperature (T_g) are shown on Table 2. Thermal expansion coefficient (α) varies between $7.58 \times 10^{-6}\ ^{\circ}C^{-1}$ and $5.85 \times 10^{-6}\ ^{\circ}C^{-1}$. For N-9 and N-18 glasses, changes of α with increasing Zr content are illustrated in Fig. 4. Obviously, all N-18 glasses have a higher thermal expansion coefficient than N-9 glasses. Moreover, with the increasing of Zr content, the thermal expansion coefficients of glass samples have a decrease to some extent.

Glass transition temperature of zirconia-doped Y–Si–Al–O–N glasses as a function of the amount of Zr concentration is given in Fig. 5. As can be seen in Fig. 5, there is a significant increase in T_g with increasing nitrogen content and a slightly decrease in T_g with increasing zirconium content. Nitrogen addition increases the cross-link density of the glass network structure by the formation of N≡ and − N= linkages. A fit of the data to a linear dependence of T_g on both N and Zr content yielded $T_g = 849 + 4.78[N] - 1.5[Zr]$ ([N] and [Zr] in eq%). The data thus indicate that the Zr content has less effect on T_g than N content.

Table 3
Heat treatment conditions (°C, h) of the zirconia-doped Y-Al-Si-O-N oxynitride glasses and the crystalline phases, Vickers hardness (H_v) and fracture toughness (K_{Ic}) of these glass-ceramics obtained after heat treatment.

Sample ID	Heat treatment conditions	Crystalline phase	H_v ($\pm$0.1 GPa)	K_{Ic} ($\pm$0.2 MPa $m^{1/2}$)
N-9 series				
Zr0N9	950 °C, 4 h+1300 °C,6 h	Mullite	9.0	1.58
Zr2N9	950 °C, 4 h+1300 °C,6 h	Mullite	9.6	1.64
Zr4N9	950 °C, 4 h+1300 °C,6 h	Mullite	10.1	1.78
Zr6N9	950 °C, 4 h+1300 °C,6 h	Mullite, zirconia yttrium oxide	9.8	1.89
N-18series				
Zr0N18	950 °C, 4 h+1300 °C,6 h	Mullite	10.2	1.85
Zr2N18	950 °C, 4 h+1300 °C,6 h	Mullite	10.5	1.96
Zr4N18	950 °C, 4 h+1300 °C,6 h	Mullite	10.7	2.12
Zr6N18	950 °C, 4 h+1300 °C,6 h	Mullite, zirconia yttrium oxide	11.0	2.27

The glass transition temperature (T_g) depends on the coordination number of elements and the bonding strength between elements in the glass. The glass transition temperature, T_g, do not depend very much on the zirconia content. The small decrease observed, however, is significant. When Zr is added to the glass compositions, the amount of other cations, Y and the network forming ions, Si and Al are all decreased slightly. Zr is likely to be an intermediate ion between network formers and modifiers in the glass structure. The combination of zirconium and oxygen leads to the increase of the number of

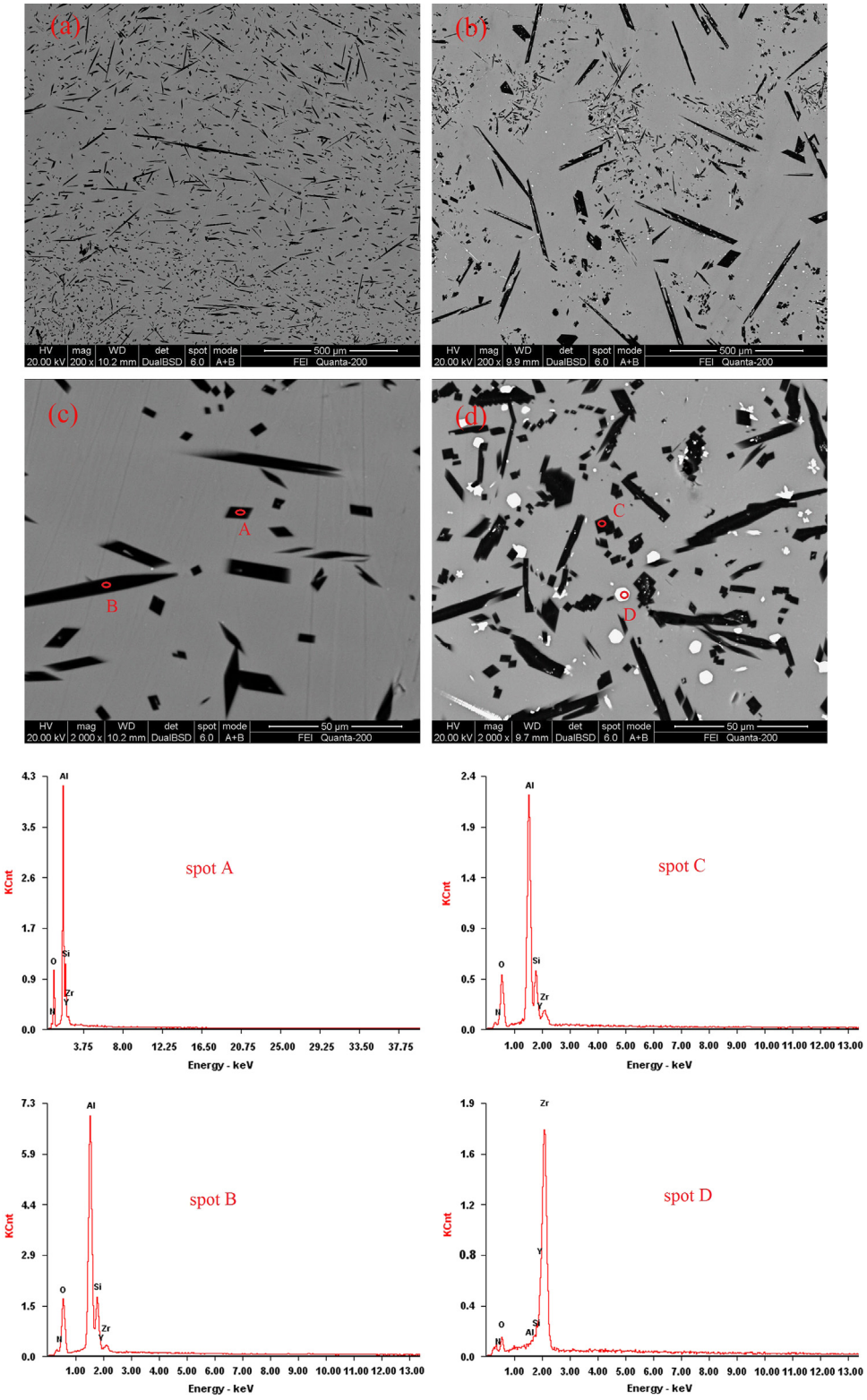

Fig. 7. SEM micrographs of the zirconia-doped Y–Si–Al–O–N oxynitride glass-ceramic samples Zr4N9 (a and c) and Zr6N18 (b and d). EDS spectra of points A–D marked in the micrographs (c) and (d).

non-bridging oxygen and the glass network is disrupted. When the nitrogen content is increasing, as previously explained, the glass network becomes more compact and rigid because of the formation of tri-coordinated nitrogen. In Fig. 4, the thermal expansion coefficients decrease from $7.58 \times 10^{-6}\ ^{\circ}C^{-1}$ to $5.85 \times 10^{-6}\ ^{\circ}C^{-1}$, however, the dependence is not linear even if data scatter of $\pm 0.05 \times 10^{-6}\ ^{\circ}C^{-1}$ is considered. The thermal expansion coefficient (α) is determined by the asymmetry of the amplitude of thermal vibrations in the glass and decreases with the rigidity of the glass network increases. However, the changes in coordination number of network former cations may cause either the increase or decrease of α depending on the effect on glass structure [22].

3.6. The crystallization data and microstructure of glass-ceramics

Following heat treatment of the glasses under flowing nitrogen at T_g+50 °C for 4 h and Tc for 6 h, the glass-ceramics produced were analyzed by XRD and SEM. Fig. 6 and Table 3 present the changes of crystalline phases in the zirconia-doped oxynitride glass-ceramics. As depicted in Fig. 6, crystalline phase identified for Zr4N9 samples was mullite ($Al_6Si_2O_{13}$), whereas for high Zr content samples (Zr6N9 and Zr6N18), peaks may be associated to mullite ($Al_6Si_2O_{13}$) and zirconia yttrium oxide ($Zr_{0.758}Y_{0.242}O_{1.879}$). Fig. 7 shows the SEM micrograph and EDS spectra of the glass-ceramic samples Zr4N9 and Zr6N18. The microstructure of the glass-ceramic Zr4N9 (heat-treated at 950 °C for 4 h and 1300 °C for 6 h) is shown in Fig. 7(a) and (c). Many black cubic and lath-shaped crystals of mullite ($Al_6Si_2O_{13}$) can be seen as the only crystalline phase. The microstructure of glass-ceramic Zr6N18 is shown in Fig. 7(b) and (d). Compared to glass-ceramic Zr4N9, a new crystalline phase zirconia yttrium oxide ($Zr_{0.758}Y_{0.242}O_{1.879}$) begins to appear and grow up. The zirconia yttrium oxide ($Zr_{0.758}Y_{0.242}O_{1.879}$) crystals are spheroidal and have a diameter of about 5 μm. However, it has not been found that partial substitution of zirconium sites in zirconia by yttrium in oxynitride glass-ceramics studied before.

3.7. Mechanical properties of the glass-ceramics

The hardness and fracture toughness values of the glass-ceramic samples are shown in Table 3. All glass samples have a higher hardness and fracture toughness after heat treatment and crystallization. The harness varies between 9.0 and 11.0 GPa while the fracture toughness varies between 1.58 and 2.27 MPa $m^{1/2}$. In Fig. 8, the fracture toughness of the glass-ceramic samples is plotted vs. the Zr content. It can be concluded that the K_{Ic} increases linearly with Zr content.

Hardness values depend on the proportions of different phases in the glass-ceramic microstructure and their crystal sizes as well as their individual hardness values [1,3]. With the increase in zirconium content in the oxynitride glass-ceramics, when the proportion of the crystallized phases (including mullite and zirconia yttrium oxide) increases compared to the residual glassy phase, there is a promotion in the hardness. The increase in the hardness of the oxynitride glass-ceramics with N content is due to an increase in the nitrogen content of the residual glass phase.

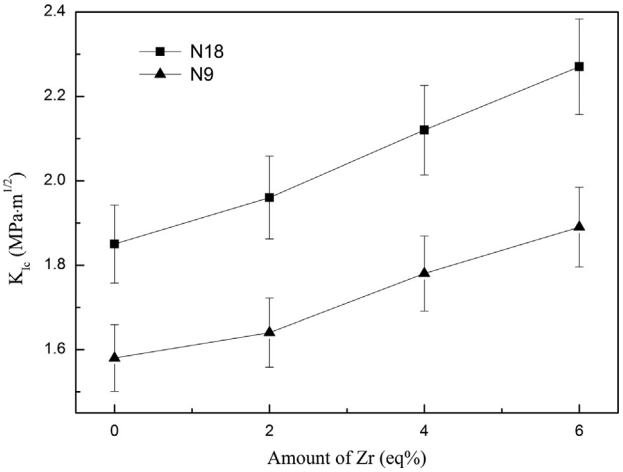

Fig. 8. Fracture toughness of the zirconia-doped Y–Si–Al–O–N oxynitride glass-ceramics as a function of amount of zirconium.

Nitrogen, as well as zirconia, was introduced into the glass-ceramics in order to improve the mechanical properties of the material. With increasing of Zr content (from 0 to 6 eq%), the fracture toughness value increases as a result of the beneficial effect of the martensitic tetragonal-to-monoclinic transformation in zirconia on toughening brittle materials [13].

4. Conclusions

The effect of ZrO_2 additions on thermal and mechanical properties and glass structure of Y–Si–Al–O–N oxynitride glasses and glass-ceramics was studied in this paper. It was found that the addition of ZrO_2 to the oxynitride glass has an effect on lowering the glass transition temperature and increasing the hardness slightly. When nitrogen content increases, density, Vickers hardness, fracture toughness and glass transition temperature values increase, whereas the thermal expansion coefficient is reduced. All the glass-ceramic samples have a higher hardness value than the glass samples, and the fracture toughness of the glass-ceramic samples increases with the zirconia content. In the samples with low Zr content, the dominant crystalline phase is mullite ($Al_6Si_2O_{13}$). When the zirconium content increases to 18 eq%, zirconia yttrium oxide ($Zr_{0.758}Y_{0.242}O_{1.879}$) crystals begin to appear and grow up.

Acknowledgment

The research was financially supported by the National Natural Science Foundation of China (No. 51272288).

References

[1] S. Hampshire, R.A.L. Drew, K.H. Jack, Viscosities, glass transition temperatures, and microhardness of Y–Si–A1–O–N glasses, Journal of the American Ceramic Society 67 (3) (1984) C46–C47.

[2] S. Hampshire, Oxynitride glasses, Journal of the European Ceramic Society 28 (7) (2008) 1475–1483.
[3] R.A.L. Drew, S. Hampshire, K.H. Jack, The preparation and properties of oxynitride glasses'', in: F.L. Riley (Ed.), Progress in Nitrogen Ceramics, Proceedings of the NATO Advanced Study Institute on Nitrogen Ceramics, held at University of Sussex, 27 July–7 August, 1981, Martinus Nijhoff, Boston, 1983, p. 323.
[4] M.A. Sainz, P. Miranzo, M.I. Osendi, Sintering behaviour and properties of YAlSiO and YAlSiON glass-ceramics, Ceramics International 37 (5) (2011) 1485–1492.
[5] D.N. Coon, T.E. Doyle, J.R. Weidner, Refractive indices of glasses in the Y–Al–Si–O–N system, Journal of Non-Crystalline Solids 108 (2) (1989) 180–186.
[6] W. Redington, A. Kidari, M. Redington, F. Laffir, M.J. Pomeroy, S. Hampshire, Origins of colour in Yb–Si–Al–O–N glasses, Journal of the European Ceramic Society 32 (7) (2012) 1359–1364.
[7] A. Kidari, C. Mercier, A. Leriche, B. Revel, M.J. Pomeroy, S. Hampshire, Synthesis and structure of Na–Li–Si–Al–P–O–N glasses prepared by melt nitridation using NH_3, Materials Letters 84 (2012) 38–40.
[8] L.J.M.G. Dortmans, D. De Graaf, US Patent Applications 11/917,906, June 20, 2006.
[9] H. Osafune, S. Kitamura, T. Kawasaki, EP Patent no. 0650937, March 5, 1997.
[10] P.F. Becher, M.J. Lance, M.K. Ferber, M.J. Hoffmann, R.L. Satet, The influence of Mg substitution for Al on the properties of SiMeRE oxynitride glasses, Journal of Non-Crystalline Solids 333 (2) (2004) 124–128.
[11] X.Y. Li, A.X. Lu, Z.H. Xiao, C.G. Zuo, The influences of cations on the properties of Y–Mg–Si–Al–O–N glasses, Journal of Non-Crystalline Solids 354 (31) (2008) 3678–3684.
[12] T. Höche, M. Deckwerth, C. Rüssel, Partial stabilization of tetragonal zirconia in oxynitride glass-ceramics, Journal of the American Ceramic Society 81 (8) (1998) 2029–2036.
[13] T. Rouxel, Y. Laurent, Fracture characteristics of SiC particle reinforced oxynitride glass using chevron-notch three-point bend specimens, International Journal of Fracture 91 (1) (1998) 83–101.
[14] P. Korgul, D.P. Thompson, The transparency of oxynitride glasses, Journal of Materials Science 28 (2) (1993) 506–512.
[15] M. Środa, C. Paluszkiewicz, The structural role of alkaline earth ions in oxyfluoride aluminosilicate glasses-infrared spectroscopy study, Vibrational Spectroscopy 48 (2) (2008) 246–250.
[16] J.J. Videau, J. Etourneau, J. Rocherulle, P. Verdier, Y. Laurent, Structural approach of sialon glasses: M–Si–Al–O–N, Journal of the European Ceramic Society 17 (15–16) (1997) 1955–1961.
[17] B. Koleva, B. Ivanova, T.U. Kolev, Linearly polarized ir spectroscopy: theory and applications for structural analysis, Taylor & Francis Group, 2012.
[18] A. Sharafat, J. Grins, S. Esmaeilzadeh, Hardness and refractive index of Ca–Si–O–N glasses,, Journal of Non-Crystalline Solids 355 (4–5) (2009) 301–304.
[19] M.J. Pomeroy, C. Mulcahy, S. Hampshire, Independent effects of nitrogen substitution for oxygen and yttrium substitution for magnesium on the properties of Mg-Y–Si–Al–O–N glasses, Journal of the American Ceramic Society 86 (3) (2003) 458–464.
[20] K. Lederer, M. Deckwerth, C. Rüssel, Zirconia-doped Mg–Ca–Al–Si–O–N glasses: preparation and properties, Journal of Non-Crystalline Solids 224 (2) (1998) 103–108.
[21] Z. Luo, G. Qu, X. Chen, X. Liu, A. Lu, Effects of nitrogen and lanthanum on the preparation and properties of La–Ca–Si–Al–O–N oxynitride glasses, Journal of Non-Crystalline Solids 361 (0) (2013) 17–25.
[22] F. Lofaj, R. Satet, M.J. Hoffmann, A.R. de Arellano-López, Thermal expansion and glass transition temperature of the rare-earth doped oxynitride glasses, Journal of the European Ceramic Society 24 (12) (2004) 3377–3385.
[23] T. Wakihara, J. Tatami, K. Komeya, T. Meguro, A. Kidari, S. Hampshire, M.J. Pomeroy, Effect of TiO_2 addition on thermal and mechanical properties of Y–Si–Al–O–N glasses, Journal of the European Ceramic Society 32 (6) (2012) 1157–1161.
[24] A. Bhatnagar, M.J. Hoffman, R.H. Dauskardt, Fracture and subcritical crack-growth behavior of Y–Si–Al–O–N glasses and Si_3N_4 ceramics, Journal of the American Ceramic Society 83 (3) (2000) 585–596.